

A NOTE ON THE FLOW OF VISCOPLASTIC MATERIALS THROUGH
COMPLEX GEOMETRIES

P. R. Souza Mendes

M. F. Naccache

H. T. M. Vinagre

M. Bosscher

Department of Mechanical Engineering

Pontifícia Universidade Católica, Rio de Janeiro, RJ 22453-900 — Brazil

Abstract

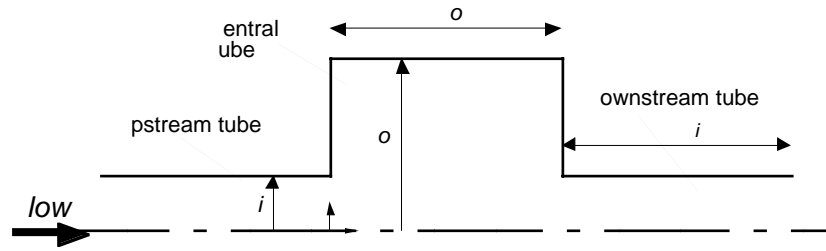
The inertialess flow of viscoplastic materials through an axisymmetric channel formed by an abrupt expansion followed by a contraction is studied. Flow visualization experiments were performed with a Carbopol aqueous solution. The rheological behavior of the solution was determined with the aid of a rotational rheometer, and it was observed that the viscosity function is well represented by the Herschel-Bulkley equation. Numerical solutions of the mass and momentum balance equations were also obtained. In these solutions it was assumed that the materials behave like a Generalized Newtonian Liquid with a biviscosity function, which mimics closely the Herschel-Bulkley equation but allows deformation below the yield stress limit. The flow visualization results showed that flow is observed only in an inner axisymmetric region whose diameter is approximately twice the one of the inlet and outlet tubes. Outside this region the flow is stagnant, and a fracture between these two regions is observed. The corresponding numerical solutions are not capable of predicting the observed flow pattern.

Keywords: Expansion flows, Contraction flows, Viscoplastic materials.

1. INTRODUCTION

This work analyzes the flow of viscoplastic materials through an abrupt axisymmetric expansion followed by an abrupt contraction, as shown in Fig. 1. Expansion and contraction flows are found in some common engineering situations, such as extrusion processes, multi-size tube flows, and other. Viscoplastic materials are present in many industrial processes. Examples of viscoplastic materials are grease, butter, paints, drilling muds, mustard, among others. The main characteristic of these materials is the presence of an yield stress. Above the yield stress the material behaves as a liquid, and, below it, as a solid. This behavior leads to an apparent fracture of the material in some complex geometries, which may have strong influence in pressure drop and heat transfer results.

The mechanical behavior of viscoplastic materials is commonly given by the Generalized Newtonian (GNL) constitutive equation (Bird et al., 1987), namely, $\boldsymbol{\tau} = \eta(\dot{\boldsymbol{\gamma}})\dot{\boldsymbol{\gamma}}$ where $\boldsymbol{\tau}$ is the extra-stress tensor, $\dot{\boldsymbol{\gamma}}$ is the rate-of-deformation tensor, defined as $\text{grad}\mathbf{v} + (\text{grad}\mathbf{v})^T$, \mathbf{v} being



Figurã : The geometry

the velocity vector and \cdot is the viscosity function, given by the Herschel-Bulkley equation (Bird et al., 1987).

1.1 Literature review

An overview of the rheology and flow of viscoplastic materials was presented by Bird et al. (1983), where some simple flow situations were analyzed. The flow of Bingham materials through tubes was analyzed in the literature by some authors (Bird et al., 1987, Vradis et al., 1992). In the core region of the tube the stress is lower than the yield value. Inside this region, called plug flow region, the fluid behaves as a solid material. The flow of Bingham materials through an 1×2 abrupt expansion was analyzed numerically by Vradis and Ötügen (1997). It was observed that the reattachment length decrease with yield stress and increase with Reynolds number. Naccache and Souza Mendes (1997) analyzed numerically the flow pattern of Bingham materials through abrupt expansions as a function of Reynolds number, yield stress and expansion ratio. It was noted that the reattachment length increases with Reynolds number, decreases with yield stress and is practically independent of the expansion ratio. An experimental study of the flow through axisymmetric expansions was performed by Pak et al (1990). This work analyzes the influence of Reynolds number on separation zones and reattachment length of Newtonian, purely viscous and viscoelastic fluids in 1×2 and 1×2.7 abrupt axisymmetric expansions. It was observed that the reattachment length for purely viscous fluids is almost the same as for Newtonian fluids. For laminar flows the effect of elasticity is to decrease the reattachment length, while in turbulent flows the opposite trend is observed.

One important discussion in the literature of viscoplastic materials is the numerical difficulty in using the von Mises yield criterion in the viscosity function. Essentially two types of modification of the Bingham viscosity function have been proposed to handle this, namely, the bi-viscosity model (Lipscomb and Denn, 1984, Gartling and Phan-Thien, 1984, O'Donovan and Tanner, 1984), and Papanastasiou's model (Papanastasiou, 1987). Both modifications have been used successfully in numerical simulations of different complex flows (e.g., Ellwood et al., 1990, Abdali et al., 1992, Beverly and Tanner, 1992, Wilson, 1993, Wilson and Taylor, 1996, Piau, 1996). Similar equations for Herschel-Bulkley viscosity function can be obtained (Macosko, 1994).

Moreover, Lipscomb and Denn (1984) observed that yielding and flow must occur everywhere in complex flows in confined geometries, which is generally inconsistent with the classic Bingham plastic model. Wilson (1983) showed that, for suitably large yield stresses, yield surfaces can exist in confined complex geometries if the biviscosity law is employed, even when the Bingham plastic limit is approached. Piau (1996) explained that, if some deformation in the plug-flow region is allowed (either elastic or viscous), yield surfaces are possible whenever there are regions of deformation (or deformation rate) low enough as to require stress levels below the yield stress to be realized.

Recently, Barnes (1999a, 1999b) performed a comprehensive review about yield stress materials, reviving the argument that yield stress actually does not exist. He shows, for a large number of materials typically classified as viscoplastic, that when careful measurements are performed below the “yield stress”, it is found that flow actually takes place, and the viscosity function looks like the bi-viscosity model. However, an apparent yield stress can exist as a useful mathematical description of limited data, over a given range of flow conditions.

The present work analyzes numerically and experimentally the inertialess flow of a viscoplastic material through an axisymmetric sudden expansion and contraction. The main goal is to evaluate the performance of the GNL constitutive equation for the flow of viscoplastic materials in this complex flow situation, by comparing the numerical predictions with flow visualization results. In the numerical simulation, the governing equations were discretized with the aid of the finite volume method. A modified bi-viscosity model was used to avoid the numerical difficulty of the Von Mises criterion. Velocity and pressure fields were obtained numerically. In the experimental study, flow visualizations for two values of the geometrical parameter are performed, for a 0.5% Carbopol aqueous solution.

2. NUMERICAL MODELING

The flow studied is steady and axisymmetric and enters the large tube with a developed velocity profile. The fluid is modeled by the GNL constitutive equation and the viscosity function is given by the Herschel-Bulkley model (Bird et al., 1987).

For the steady flow of a viscoplastic material through a duct, the dimensionless mass and momentum equations are:

$$\text{div}^0 \mathbf{v} = 0 \quad (1)$$

$$\text{grad}^0 \phi^0 = -\text{grad}^0 p^0 + \frac{2\eta^0}{Re} \text{div}^0 (\text{grad}^0 \mathbf{v}^0) \quad (2)$$

where $\mathbf{v}^0 = \mathbf{v} = R_{i,c} \mathbf{e}_i$ and $p^0 = p = \frac{\rho c}{2} (R_{i,c})^2$. The dimensionless coordinates are $x^0 = x = R_i$ and $r^0 = r = R_i$. The characteristic shear rate $\dot{\gamma}_c$ is taken as equal to the developed value of the shear rate at tube wall at the upstream tube, given by (Soares et al., 1997):

$$\dot{\gamma}_c = \frac{\dot{\gamma}_{R_i, \text{fil}}}{K} = \frac{\eta}{R_i} \frac{n+1}{2n} \left[\frac{1}{2} (1 + r_0^0) + \frac{n}{2n+1} r_0^0 (1 + r_0^0)^2 + \frac{n}{3n+1} (1 + r_0^0)^3 \right]^{1/n} \quad (3)$$

In this equation $r_0^0 = \dot{\gamma}_0^0 = \dot{\gamma}_0 = \dot{\gamma}_{R_i}$ is the dimensionless yield stress. The quantities $\dot{\gamma}_{R_i}$, η and R_i are the shear stress at wall, mean velocity and radius of the smaller tube (radius R_i), respectively. The characteristic viscosity is chosen as the viscosity at the characteristic shear rate, $\eta_c = \eta(\dot{\gamma}_c)$ and the Reynolds number is defined as $Re = \frac{2\eta_c R_i}{\rho c}$.

The boundary conditions are the usual no-slip condition at walls, the symmetry condition at the centerline and locally parabolic flow at the outlet. The flow was solved only for the central and the downstream tubes. At the inlet of the central tube, the flow was considered hydrodynamically developed and the velocity profile is given by:

$$u_{R_i, \text{fil}}^0(r^0) = \begin{cases} \frac{n}{n+1} \left[\frac{1}{1+r_0^0} \right]^{1/n} (1+r_0^0)^{\frac{n+1}{n}} - (r^0 + r_0^0)^{\frac{n+1}{n}} & \text{if } r^0 > r_0^0 \\ \frac{n}{n+1} (1+r_0^0) & \text{if } r^0 < r_0^0 \end{cases} \quad (4)$$

As discussed previously, a modified bi-viscosity model was used for the viscosity function:

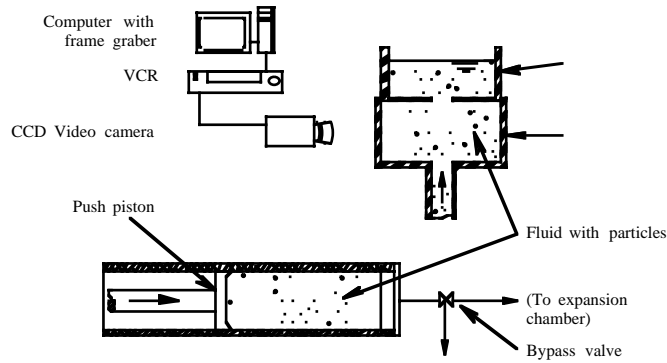


Figure 2: Schematic of the experimental apparatus

$$\mu_0 = \begin{cases} \frac{\dot{\gamma}_0^0}{\dot{\gamma}_{large}^0} + (1 - \frac{\dot{\gamma}_0^0}{\dot{\gamma}_{large}^0})^{-n_i} & \text{if } \dot{\gamma}_0^0 > \dot{\gamma}_{small}^0 \\ \dot{\gamma}_{large}^0 & \text{otherwise} \end{cases} \quad (5)$$

where $\dot{\gamma}_0^0 = \dot{\gamma}_c$, $\dot{\gamma}_{large}^0 = \dot{\gamma}_c$ and $\dot{\gamma}_{small}^0 = \dot{\gamma}_{R_i}$ are the dimensionless shear rate, viscosity and yield stress, respectively. We adopted $\dot{\gamma}_{large}^0 = 1000$ (Beverly and Tanner, 1992). Then, $\dot{\gamma}_{small}^0 = \dot{\gamma}_0^0 (1 - \frac{\dot{\gamma}_0^0}{\dot{\gamma}_{large}^0})^{1/n_i}$, $\dot{\gamma}_0^0 = 1000$

2.1 Numerical solution

The conservation equations of mass and momentum are discretized by the finite-volume method described by Patankar (1980). Although the Reynolds number values were kept below 0.01 for all cases, the inertia terms were kept in the momentum equations. Staggered velocity components are employed to avoid unrealistic pressure fields. The SIMPLE algorithm (Patankar, 1980) was used, in order to couple the pressure and velocity. The resulting algebraic system is solved by the TDMA line-by-line algorithm (Patankar, 1980) with the block correction algorithm (Settari and Aziz, 1973) to increase the convergence rate.

The mesh utilized is uniform per zones in the axial and radial directions. For the cases with $L_0 = D_0 = 0.5$, a 102×82 mesh was used and for the other cases the mesh used was equal to 122×82 . The downstream tube length was fixed equal to $10R_i$, in order to avoid the influence of the outlet boundary on the flow. To validate the numerical solution, some tests are performed. The error obtained for the product of the friction factor and the Reynolds number with respect to the exact value ($fRe = 8 \ln D = \gamma$), for a fully developed Newtonian flow at the downstream tube was equal to 5%, while for the Herschel-Bulkley material the error was always less than 2%.

3. EXPERIMENTAL APPARATUS

A schematic view of the experimental apparatus is shown in Fig. 2. A single-piston/cylinder pump was used to drive the flow through the transparent plexiglas-made expansion/contraction. The transparent fluid was mixed with light reflective particles to allow the flow visualization. The flow of the particle-laden fluid was recorded. Afterwards, the movie was digitized and the images processed with a computer. The particles were highlighted and the background removed with software to obtain the streamlines.

The pumping system consists of an actuator that pushes a piston in a cylinder. The two Aluminum cylinders used are 600 mm long and have diameters of 57.3 mm and 12.7 mm. The corresponding flow rates are respectively $361 \text{ mm}^3/\text{s}$ for the viscoplastic fluid and $17.7 \text{ mm}^3/\text{s}$ for the Newtonian case. The Reynolds number of the flow was kept below 0.01 for all cases, to assure no inertial effects. A bypass valve was used to remove air bubbles from the transparent

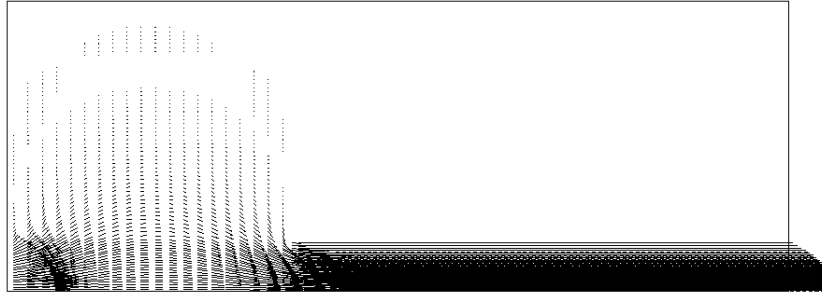


Figure 3: Velocity vectors $\alpha_0 = 0$ (Newtonian) $L_o/D_o = 0.5$

manifold before starting the videotape.

The expansion/contraction chamber was made of 57.7 mm diameter transparent plexiglas tube and has an overflow chamber on top to hold the fluid. The flow was vertical and upwards. We used a black and white CCD camera, model KP-M1 (Hitachi Denshi, Ltda.), coupled to either a 12.5-75 mm /f1.8 (Toyo Optics, Japan) or a 18-108mm/f2.5 (Computar, Japan) zoom lens, connected to a good quality standard VCR. The light source is a 300 W Kodak Ecktagraphic IIIE-plus slide projector (Kodak Company, USA). In the projector slide chamber, an Aluminum slide 1.6 mm thick and having a 1.1 mm wide vertical slot was used to create a plane of light about 2 mm wide. The camera was positioned perpendicular to this plane of light. The videotape was digitized with a Power Mac 8500/120 (Apple Computer Inc.) and the public domain NIH Image v. 1.6.1 program (National Institutes of Health USA).

3.1 Fluids

The measurements were done for two different fluids, a polymeric aqueous solution (viscoplastic) and a polyethylene glycol (Newtonian). All concentrations were measured by weight. The 0.5% Carbopol 676 (B. F. Goodrich Chemical Co., USA) aqueous solution was neutralized with 0.04% Sodium Hydroxide (Rhos Ltda., Brazil). The viscosity of this solution is highly dependent on its pH, which was kept at a value of 6.0. The viscosity for this solution was observed to decrease sharply with increasing shear rate. For the Carbopol solution both the viscosity and shear stress fit well to a Herschel-Bulkley model. The rheological properties obtained using a rotational rheometer (Physica UDS 200) are $\tau_0 = 78.3 \text{ Pa}$ and $K = 111 \text{ Pa}\cdot\text{s}$ and $n = 0.4$. The fluid density is essentially equal to that of water, i.e., $\rho = 1000 \text{ kg/m}^3$. For the Newtonian fluid we used an aqueous solution of 55% polyethylene glycol (Polietileno glicol 6000, Vetec Ltda., Brazil). This concentration is close to the saturation point at room temperature. We measured the viscosity of this solution and found a constant value for a wide range of shear rates. The density was found to be 1090 kg/m^3 for this Newtonian solution. Both solutions were transparent, and the visualization was possible by mixing light reflecting Pliolite particles (GoodYear Inc, USA) in the solutions. The particle diameters were between 149 and 250 μm and the concentrations in the solutions ranged between 0.08 and 0.12%.

4. RESULTS AND DISCUSSION

As stated earlier, all the numerical and experimental results obtained pertain to negligible inertia ($Re = \rho \omega D_c < 1 \times 10^2$). Two different values of the ratio L_o/D_o were analyzed, viz. $L_o/D_o = 0.5$ and 1. The results for larger values of L_o/D_o are qualitatively similar to the ones obtained for $L_o/D_o = 1$.

Figures 3–5 show the velocity vectors obtained numerically for $L_o/D_o = 0.5$ and for $\alpha_0 = 0$ (Newtonian) 0.4 and 0.7. The flow patterns observed show an interesting structure. In the downstream tube (radius R_i), the core region is the region of lowest velocity gradients, and hence

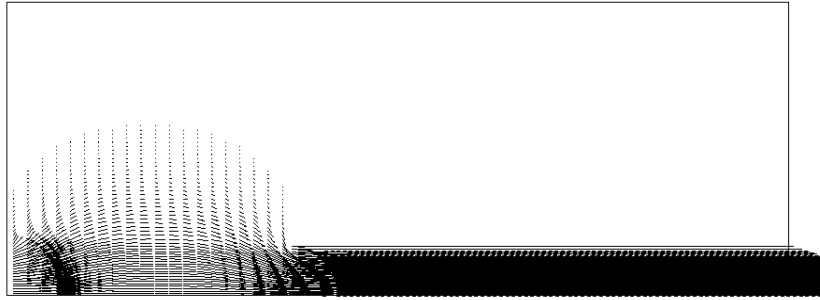


Figure 4: Velocity vectors $\alpha_0^0 = 0.14; L/D = 0.5$

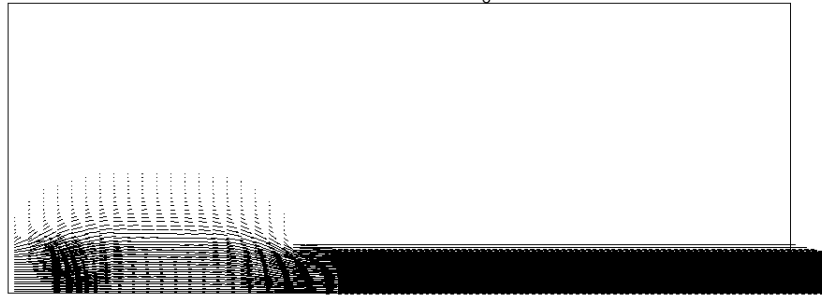


Figure 5: Velocity vectors $\alpha_0^0 = 0.7; L/D = 0.5$

of lowest stresses. Near the wall, the velocity gradient is larger, and so is the stress. Therefore, the centerline region is a region where the stress is lower than the yield stress, and the material move as a solid body. This region is called the plug flow region. The plug flow region increases with the yield stress, as it can be seen in Figs. 3–5 and 7–9. In the large duct (radius R_o), the plug region close to the centerline is also present, except close to the expansion and contraction planes, where the velocity gradients are high. Away from the centerline and adjacent to the tube wall, there is a region where the velocities are rather small, leading to small velocity gradients and stresses lower than the yield stress. The non-zero but small velocities in this region is consistent with the bi-viscosity model. It can be noted that the nearly-stagnant region increases with the yield stress, as expected. For the Newtonian case, negative values of the velocity indicate a slow recirculating flow in this region.

Flow visualizations for the viscoplastic material for $L_o=D_o = 0.5$ and 1 are shown in Fig. 6. It can be observed that there is no flow in a large region adjacent to the wall for $L_o=D_o = 0.5$ (left picture). Furthermore, from the movie it can be observed that the velocity profile is rather flat the core region, with a steep decrease to zero towards the stagnant region. Within our limited observations, it looks like the velocity profile is discontinuous, i.e., as if internal slip occurs. This behavior is qualitatively different from that one inferred from the numerical solution, where the velocity smoothly decreases to zero near this limiting region. Moreover, the stagnant region observed experimentally is significantly larger than the one predicted by the numerical approach. For the Newtonian liquid, we have been facing problems of operational nature, and flow visualization results are not yet available.



Figure 6: Experimental streamlines for the viscoplastic liquid $\alpha_0^0 = 0.14; L/D = 0.5$ and 1

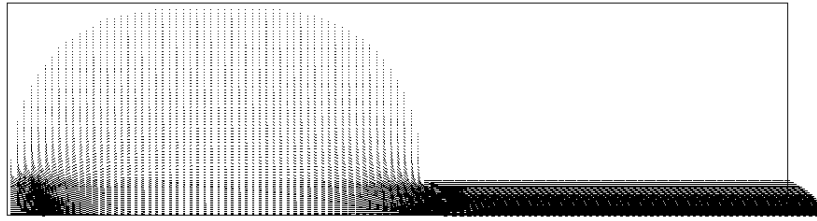


Figure 7: Velocity vectors $r_o^0 = 0$ (Newtonian); $L_o = D_o = 1$

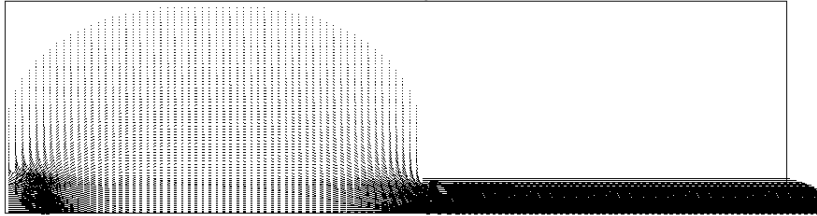


Figure 8: Velocity vectors $r_o^0 = 0.14$; $L_o = D_o = 1$

The velocity vectors for $L_o = D_o = 1$ and for $r_o^0 = 0$ (Newtonian) and 0.14 and 0.7 are shown in Figs. 7–9. Flow patterns obtained experimentally for the viscoplastic material and $L_o = D_o = 1$ is shown in Fig. 6. It can be observed that the flow patterns are different from that ones obtained for $L_o = D_o = 0.5$. In these cases, all the fluids flow in similar patterns, with no stagnant region, not even for the viscoplastic materials. For this case, the numerical and experimental observations are in good agreement.

5. CONCLUSIONS

This paper investigates the performance of the GNL constitutive equation for the flow of viscoplastic materials in a complex geometry, namely, an axisymmetric duct consisting of an expansion followed by a contraction. The governing equations of mass and momentum are solved numerically via a finite-volume technique. The numerical solution gives the velocity, viscosity and pressure fields. The flow pattern was also obtained experimentally.

It is observed that the flow pattern obtained numerically with the bi-viscosity model agree well with the experimental ones only for larger values of $L_o = D_o$. Experimental observations indicate that there is a flow pattern transition for $L_o = D_o < 1$. Below this value, the viscoplastic material starts to fracture near the core region of the flow. The numerical solution was not able to predict this behavior. The results obtained numerically give a smooth velocity profile through the radius of the duct. For $L_o = D_o > 1$ all the materials yield the same qualitative flow pattern, no fracture being observed. The numerical predictions for this case are in good agreement with the experimental observations.

ACKNOWLEDGEMENTS

Financial support for the present research was provided by CNPq and MCT.

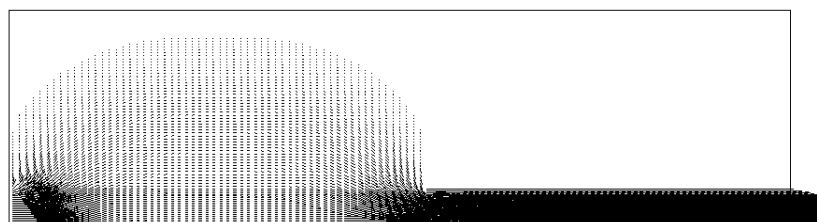


Figure 9: Velocity vectors $r_o^0 = 0.7$; $L_o = D_o = 1$

REFERENCES

- † Abdali, S.S., Mitsoulis, E. and Markatos, N.C., 1992, “Entry and exit flows of Bingham fluids”, *J. Rheology*, V. 36, pp. 389.
- † Barnes, H.A., 1999a, “A brief history of the yield stress”, *Appl. Rheol.*, V. 9 (6), pp. 262–266.
- † Barnes, H.A., 1999b, “Yield stress – a review, or ...fi 3 çfi%† – everything flows?”, *J. Non-Newtonian Fluid Mech.*, V. 81, pp. 133.
- † Bird, R.B., Armstrong, R.C. and Hassager, O., 1987, “Dynamics of Polymeric Liquids”, Ed. Wiley.
- † Bird, R.B., Dai, G.C. and Yarusso, B.J., 1983, “The rheology of flows of viscoplastic materials”, *Rev. Chem. Eng.*, V. 1, pp.1–70.
- † Beverly, C.R. and Tanner, R.I., 1992, “Numerical analysis of three-dimensional Bingham plastic flow”, *J. Non-Newtonian Fluid Mechanics* , V. 42, pp.85–115.
- † Ellwood, K.R.J., Georgiou, G.C., Papanastasiou, C.J. and Wilkes, J.O., 1990, “Laminar jets of Bingham-plastic liquids”, *J. Rheol.*, V. 34, pp.787–812.
- † Gartling, D.K. and Phan-Thien, N., 1984, “A numerical simulation of a plastic fluid in a parallel-plate plastometer”, *J. Non-Newt. Fluid Mech.* , V. 14, pp.347–360.
- † Lipscomb, G.G. and Denn, M.M., 1984, “Flow of Bingham fluids in complex geometries”, *J. Non-Newt. Fluid Mech.* , V. 14, pp.337–346.
- † Macosko, C.W., 1994, “Rheology: Principles, Measurements, and Applications”, Ed. VCH.
- † Naccache, M.F. and Souza Mendes, P.R., 1997, “Abrupt Expansion Flows of Bingham Materials”, XIV Congresso Brasileiro de Engenharia Mecânica, CDROM.
- † O’Donovan, E.J. and Tanner, R.I., 1984, “Numerical study of the Bingham squeeze film problem”, *J. Non-Newt. Fluid Mech.* , V. 15, pp.75–83.
- † Pak, B., Cho, Y.I. and Choi, S.U.S., 1990, “Separation & Reattachment of Non-Newtonian Fluid Flows in a Sudden Expansion Pipe”, *J. Non-Newt. Fluid Mech.* , V. 37, pp.175–199.
- † Papanastasiou, T.C., 1987, “Flows of materials with yield”, *J. Rheol.* , V. 31, pp.385–404.
- † Patankar, S. V., 1980, “Numerical Heat Transfer & Fluid Flow”, Hemisphere Pub. Corp..
- † Piau, J.M., 1996, “Flow of a yield stress fluid in a long domain. Application to flow on an inclined plane”, *J. Rheol.* , V. 40, pp.711–723.
- † Settari, S. and Aziz, K. , 1973, “A Generalization of the Additive Correction Methods for the Iterative Solution of Matrix Equations”, *SIAM J. Num. Anal.* , V. 10, pp.506–521.
- † Soares, M., Souza Mendes, P.R. and Naccache, M.F., 1997, “Heat Transfer to Viscoplastic Fluids in Laminar Flow Through Isothermal Short Tubes”, *Revista Brasileira de Ciências Mecânicas*, V. XIX (1), pp.1–14.
- † Vradis, G. C., Dougher, J. and Kumar, S., 1992, “Entrance pipe flow and heat transfer for a Bingham plastic”, *Int. J. Heat Mass Transfer* , V. 35, pp.543–552.
- † Vradis, G. C. and Ötügen, M. V., 1997, “The Axisymmetric Sudden Expansion Flow of a Non-Newtonian Viscoplastic Fluid”, *J. of Fluids Engineering* , V. 110, pp.193–200.
- † Wilson, S.D.R., 1993, “Squeezing flow of a yield-stress fluid in a wedge of slowly-varying angle”, *J. Non-Newt. Fluid Mech.* , V. 50, pp.45–63.
- † Wilson, S. D. R. and Taylor, A. J. , 1996, “The channel entry problem for a yield stress fluid”, *J. Non-Newt. Fluid Mech.* , V. 65, pp.165–176.